Biomass Conversion and Biorefinery
https://doi.org/10.1007/s13399-023-04553-7

ORIGINAL ARTICLE

Suppressing the formation of N-heteroaromatics during hydrothermal liquefaction of proteinaceous model feedstock

Joscha Zimmermann[1] · **Klaus Raffelt**[1] · **Nicolaus Dahmen**[1]

Received: 8 April 2023 / Revised: 20 June 2023 / Accepted: 25 June 2023

Abstract
Hydrothermal liquefaction was applied to model mixtures containing lard oil (lipid), cellulose (carbohydrate), and bovine serum albumin (protein), representing biogenic organic waste feedstocks. The content of protein was kept constant for every experiment, while the lipid and cellulose content was changed, which is expressed by the lipid to protein (LtoP) or cellulose to protein (CtoP) ratio. The reactions were conducted at 350 °C with a residence time of 20 min in 25 ml micro autoclaves. Afterwards, the lumped recovery of carbon and nitrogen into the different product phases was investigated and representative compounds were identified to get an overview of the composition on a molecular level. A high LtoP ratio results in an increased biocrude yield and eventually higher carbon recovery, while the nitrogen recovery is slightly lowered. The formation of nitrogen containing heteroaromatic species could be suppressed by the addition of lipids from 6.10 to 0.03% for pyrazines and 2.69 to 0.43% for indoles. Consequently, the formation and nitrogen recovery by heteroaliphatic amide species increased from 0.00 to 8.77%. Different reaction pathways for the formation of the different species are proposed. It turned out that reactive amine from protein degradation can be "trapped" in stable amides, preventing the formation of nitrogen heteroaromatics with oxygenated from carbohydrates.

Keywords Nitrogen · Lipids · Carbohydrates · Proteins · N-heteroaromatics

1 Introduction

Due to the rapid increase in global energy demand along with climate change issues, biomass gained interest as an alternative, carbon–neutral source for the production of chemical energy carriers. Bio-based residuals or waste feedstocks are of high interest as they need to be managed anyhow and are not included in the "fuel vs food" discussion [1]. Sewage sludge, manure, or municipal organic waste are examples for kind of cheap waste biomass, often containing a high moisture content. Hydrothermal liquefaction (HTL) is a promising technology which uses water as a heat carrier, solvent, and catalyst at the same time, avoiding pre-drying and making it suitable for a wide variety of feedstocks [2]. Elevated temperatures between 200 and 400 °C under the corresponding saturation pressure are applied to utilize the superior ionic product and a low dielectric permittivity of water, enhancing acid/base and ionic reactions [3]. With this higher reactivity, functional groups are attacked in the biogenic molecules in the organic waste. Usually, a mixture of natural polymers and other large molecules like polysaccharides, proteins, and lipids are contained in the mixture, which needs to be depolymerized and converted into smaller molecules to utilize them in downstream refining processes. The intermediate product obtained by HTL for biofuel purposes consists of a mixture of different compounds and is often referred to as biocrude [4]. This organic product contains less polar substances; therefore, side products are carbon dioxide rich gas, and aqueous phase containing the more polar components with a low molecular weight [5, 6]. Another side product occurs from re-polymerization as a solid, char-like material [7].

The usually high heteroatom content of oxygen (O) in carbohydrates and lipids is transferred into the final product phases. Considering the utilization of protein-rich waste biomass, nitrogen (N) is an additional concern if hydrocarbon fuels are the target product. Biocrude is therefore an intermediate along the process chain to fuel [8]. Extensive

✉ Klaus Raffelt
klaus.raffelt@kit.edu

[1] Institute of Catalysis Research and Technology, Karlsruhe Institute of Technology, Eggenstein-Leopoldshafen, Germany

Published online: 21 July 2023

upgrading is needed to remove heteroatoms and to improve fuel properties to reach industrial standards in the aimed application. This refining consists usually of a catalytic hydrotreatment coupled with distillation for fractionation into the different fuel cuts [9]. Hydrodeoxygenation (HDO) and hydrodenitrogenation (HDN) of the biocrude are conducted like in the processes developed for fossil crude oil, but are still under research, considering the huge concentrations of heteroatoms to deal with. Both HDO and HDN are occurring simultaneously and are competitive reactions [9]. Generally speaking, HDN is often referred to as the slower reaction mechanism, of course depending on the chemical feed composition [10, 11]. Removing heteroatoms from heterocyclic and heteroaromatic compounds is difficult as full hydrogenation and subsequent ring-opening are presumed [12]. Furthermore, Choudhary et al. showed an inhibiting effect on HDN in heavy crude fuel with high contents of polyaromatic compounds, as the latter are hydrogenated before [13]. N-heteroaromatics species are suspected to complex inorganic elements like iron, which are problematic for active catalyst sides, requiring an additional refinement for the biocrude [14, 15]. Otherwise, aliphatic amides seemingly are easier to process during HDN, as shown experimentally by Kohansal et al. for the hydrotreatment of biocrude produced from food waste [16]. Therefore, the N-content in biocrude needs to be distinguished between N-heteroaromatic and N-aliphatic compounds.

Several studies showed the influence of the organic feedstock composition on the HTL process and the biocrude composition. Fan et al. demonstrated that Maillard reactions lead to increased biocrude yields for hydrothermal conversion of the model substances lactose and lysine as more nonpolar reaction products are formed [17]. Accordingly, the N-content in the biocrude increased, eventually leading to a lower quality due to more N-heterocyclic compounds. Posmiak et al. used model substances as well in different combinations at different reaction temperatures and time [18]. Not only the beneficial effect of carbohydrates and proteins, regarding the yield, is highlighted, but also the ternary combination with lipids is introduced. The addition of lipids to the carbohydrate/protein mixture was found to improve the biocrude yield and quality. Yoo et al. tested HTL on two different microalgae strains with low or high lipid content [19]. When the focus lay on the production of transportation fuels, the high-lipid microalgae performed better in terms of biocrude yield, quality, and energy efficiency. In a comparable experiment, Feng et al. used two algae strains with different lipid contents, finding a higher biocrude yield and more N-heterocyclic compounds in the biocrude derived from the low-lipid strain [20]. A pre-treatment, removing carbohydrates from the algae matrix was proposed, lowering the generation of N-heteroaromatics. In our previous work, we successfully pre-treated sewage sludge with water and different acidic solutions at 150 °C, intending to solubilize proteins, eventually lowering the N-content in the feedstock and the resulting biocrude [21]. As lipids accumulated and proteins and carbohydrate were get washed out in the first step, the resulting biocrude showed higher yields and lower N-contents and fewer N-heterocycles. A study conducted by Croce et al. described in detail the chemical composition of biocrude obtained from different model substances and mixtures [22]. With high resolving mass spectroscopy, the composition of the biocrude derived from binary carbohydrate/protein and ternary mixtures including additional lipids was investigated. Among others, it could be shown that N-compounds differ between aliphatic amides and a large variety of heteroaromatics by the applied feedstock composition, proposing the more detailed examination of different feedstock combinations and changing ratios. In another recent study, the composition of lipid, protein, and carbohydrate was varied by different preparations of artificial food waste slurries, to see an effect on the generation of N-species [23]. A strong influence of reactive N-intermediates on the generation of heteroaromatic species was observed and supported by the development of a thermodynamic model.

In this study, our objective is to effectively reduce the formation of N-heterocyclic compounds, particularly in the aromatic form, in the biocrude obtained through HTL. Building upon previous research conducted by Fan and colleagues within our institute, which highlighted the substantial influence of lipids on the generation of these troublesome nitrogen species, we introduce a novel ternary model system [24]. This system comprises lipids (lard oil), carbohydrates (cellulose), and proteins (bovine serum albumin) and is subjected to conversion under hydrothermal conditions at 350 °C and 20 MPa. The novelty of our work lies in the deliberate and systematic variation of the lipid-to-protein ratio while maintaining a constant protein content. Through this approach, we investigate the relationship between the distribution of nitrogen among representative species in the resulting biocrude and the lipid-to-protein ratio. Such exploration enables us to identify the key pathways responsible for the formation of N-heteroaromatic compounds and propose potential strategies to suppress their generation. Additionally, in a subsequent experimental setup, we explore the impact of replacing de-ionized water with a 0.5 wt.% propionic acid solution, providing further insights into the effects of this short-chain carboxylic acid on the investigated factors.

2 Material and methods

2.1 Materials

The substances for the model feedstock mixture lard oil, cellulose, bovine serum albumin (BSA), and propionic

acid were purchased from Merck and were used without further treatment. Solvents like dichloromethane and tetrahydrofuran were obtained in chromatographic grade from Merck. Standards for GC–MS calibration like 2 piperdone, N-methylsuccinimde, 2-methylpyrazine, 2,6-dimethylpyrazine, indole, 2-methylindole, 2,3-dimethylindole quinoline, 2-methylquinoline, and 2,6-dimethylquinoline were purchased from Alfa Aesar. The fatty acid amide derivates hexadecanamide and ocatadecanamide were obtained from Cayman Chemicals.

2.2 Hydrothermal liquefaction experiments and sample collection

Seven different feedstock mixtures were prepared; while the protein content was kept constant, the cellulose and lipid content was varied. The resulting mixtures were named according to their lipid to protein weight ratio (LtoP ratio), which varied by $0.00 \leq \text{LtoP} \geq 2.00$. In a second series of experiments with LtoP ratio between 0.00 and 1.00, the aqueous solvent contained 0.5 wt.% propionic. An overview of all experiments with the given concentrations of lipid, cellulose, and protein are given in Table 1.

The HTL experiments were conducted in 25 ml autoclaves (Stainless steel, EN 1.4571). The vessels were loaded with the different organic feedstock mixtures and with 15 ml of de-ionized water to result in an organic weight fraction of 10 wt.%. Solid feedstock materials, namely cellulose and BSA, were introduced into the system using a spatula, while liquid lard oil was added using a pipette. Following this, a volume of 10 ml of de-ionized water was gradually incorporated into the mixture under continuous manual stirring with the spatula. Afterwards, the remaining 5 ml of water was used to rinse the spatula. In order to ensure uniform wetting of the solid materials, the sealed microreactors were subjected to ultrasonic treatment in a bath for a duration of 5 min. The headspace was purged with nitrogen three times and pressurized to 1 MPa before the autoclaves were sealed with a torque key. In one setup, six autoclaves were placed into a fluidised sand bath at 350 °C (SBL 2; Techne). According to the gas saturation pressure of water and the available volume, this results in a pressure of 20 MPa during the reaction [25]. The heating rate inside the autoclave was measured previously and averaged at 40 °C·min^{-1}, resulting in a heating time of 8.75 min. After the reaction temperature was reached, the autoclaves remain in the sand bath for 20 min. To stop the reaction, the reactors were removed from the sand bath and rapidly cooled down in a water bath for 10 min. The pressurized autoclaves were opened in a gas-tight containment and the released reaction gas was discarded. The liquid content and the open vessel were rinsed with 5 ml of dichloromethane (DCM) and filtered by a Büchner funnel with filter paper of 0.45 µm pore size. The same procedure was repeated four times. Solids retained on the filter were dried at 105 °C overnight and stored for further analysis. The DCM extract was stored in a refrigerator, letting the heavier organic-rich biocrude phase separate from the lighter aqueous phase. The next day, the two phases were separated by aspiration, an aqueous aliquot was collected for further analysis while the DCM of the biocrude phase was evaporated under a mild nitrogen stream overnight.

Table 1 Feedstock model mixtures experimental setup

Protein [g]	Lipid [g]	Cellulose [g]	LtoP ratio	Experimental series	
				De-ionized water	0.5 wt.% Propionic acid
0.50	0.00	1.00	0.00	4	3
0.50	0.17	0.83	0.34	1	3
0.50	0.33	0.67	0.66	1	3
0.50	0.50	0.50	1.00	3	3
0.50	0.67	0.33	1.34	1	-
0.50	0.83	0.17	1.66	1	-
0.50	1.00	0.00	2.00	4	-

2.3 Analysis

The HTL-feedstocks consisting of model substances and reaction products biocrude and residual solids were analyzed for their elemental composition using a CHNS-Analyzer (Vario EL cube, Elementar Analysetechnik GmbH, Hanau, Germany).

The aqueous phase including solubilized organics was tested by total organic carbon (TOC) and total nitrogen bound (TNb) analyzer (DIMATOC 2100 and DIMA-N, Dimatec Analysetechnik GmbH, Essen, Germany).

To identify and quantitate representative N-heteroatomic compounds in the biocrude samples gas chromatography (GC) coupled with mass spectrometry (MS) using electron impact ionization (EI) was applied. As a stationary phase, a Rxi-5MS column with 30 m × 0.32 mm × 0.25 µm (Restek Corporation, Bellefonte, PA, USA) was used. A quantity of 50 mg of samples was dissolved in 0.5 ml of tetrahydrofuran and, subsequently, prepared in a 1:100 dilution. 0.5 µL of this solution was injected at 280 °C in 1:20 split mode, using helium as carrier gas (1.5 mL·min^{-1}). The temperature program of the oven started at 70 °C holding for 2 min and then heating to 180 °C with a heating rate of 8 °C·min^{-1}, increasing again up to 280 °C with a rate of 4 °C·min^{-1} and holding there for 15 min. The temperature of the transfer line to the detector was kept at 280 °C, and the ion source to 230 °C. Qualitative analysis was conducted with a scan of the total ion current (TIC) chromatogram. Scan rate was set at 3.9 scans·s^{-1}

over a mass charge to charge ratio range of 35–400 m/z. Agilents "Unknown Analysis" software and NIST17 Database was used for identification with an applied match factor of 75%. The selected ion monitoring (SIM) mode was applied to acquire high-quality mass spectra for externally calibrated indole, quinolone, succinimide, piperidone, and amide derivates. The compounds with their responding characteristic qualifier and quantifier ions, as well as calibration curves, are listed in S2.

The structural behavior of the solid residues generated from model substances was additionally analyzed by 13C-MAS NMR. The spectra were acquired by using a JEOL 400 MHz unit equipped with a 9.4 T Oxford magnet for solid state (wide-bore) using 4 mm zirconia rotors spinning at a MAS frequency (nMAS) of 15 kHz.

2.4 Data evaluation and visualization

The yield (Y_i) of biocrude and solid residue was calculated by the following equation:

$$Y_i = \frac{m_i}{m_f} \cdot 100$$

where m_i and m_f are the mass of the product and feedstock mixture, respectively.

The element recovery into a certain HTL-product phase was calculated by the following equation:

$$ElementRecovery_i = \frac{m_i \cdot E_i}{m_f \cdot E_f} \cdot 100$$

The element recovery means the recovery of carbon or nitrogen, the index i is indicating the biocrude, aqueous, or solid product phase, m_i and m_f are the masses of the feedstock mixture where as E_i and E_f are the elemental content of the feedstock mixture.

A change indicator (CI) was calculated to evaluate the effect of propionic acid on the nitrogen recovery in representative heteroatom species. The CI compares the N-recovery of a specific species in the biocrude with and without the addition of propionic acid. If the CI value is negative, a lower N-recovery is obtained. A positive CI value indicates a higher N-recovery of such species when adding propionic acid to the feed mixture.

$$\mathrm{CI}_i = \frac{\mathrm{N.rec.}_{i,propionicacid} - \mathrm{N.rec.}_{i,deionizedwater}}{\mathrm{N.rec.}_{i,deionizedwater}}$$

where the index i denotes the N-heteroatom species; $\mathrm{N.rec.}_{i,deionizedwater}$ is the N-recovery of the species i in the biocrude derived in de-ionized water and $\mathrm{N.rec.}_{i,propionicacid}$ is the N-recovery of the species i in the biocrude derived in the aqueous propionic acid solution.

Evaluation of the fitted curves and their ANOVA was obtained in DesignExpert v8.0.6 (State-Ease, Minneapolis, MI, USA). The ANOVAs and plots of residuals are shown in the Supplementary Material, S1. For data processing and plotting the Python libraries Numpy, Pandas and Matplotlib were used. Chemical structures were drawn in ChemDraw professional 16.0. BSA and peptide structure were obtained from the SWISS-MODELL database [26].

3 Results and discussion

3.1 Biocrude and solid yield

The yields of the biocrude and the solid products after hydrothermal treatment of the model mixtures with different lipid-to-protein ratio are shown in Fig. 1. Additionally, the ratio of solid to biocrude product expressed in percentage is given. At the smallest LtoP ratio, the biocrude yield shows its lowest value of 34.3 wt.%, while the highest solid yield was obtained at 5.99 wt.%. Correspondingly, the biocrude yield increases up to a value of 66.2 wt.% at a LtoP of 2.00. At the same time, the solid yield significantly decreases to 0.54 wt.%. This can also be expressed by the solid to biocrude ratio, illustrated by the fitted, dashed curve as a function over the LtoP ratio in the figure. At a minimum ratio, the solid accounts in proportion to the biocrude 19.30 and decreased to almost half (10.90%), when the LtoP ratio was 0.33. Following

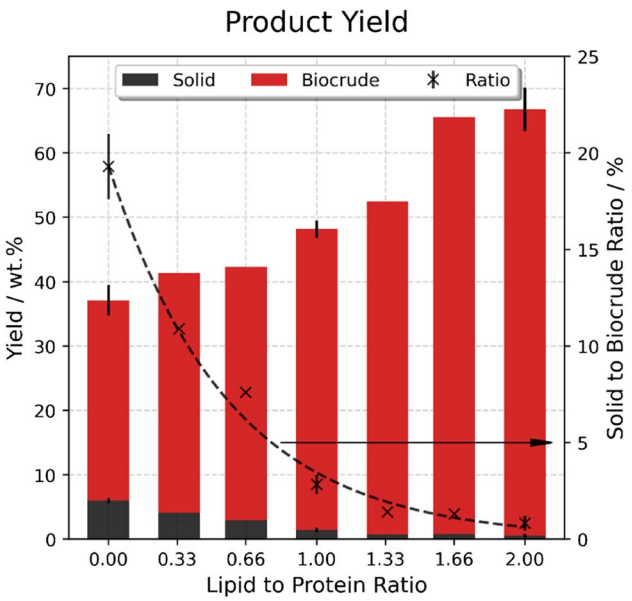

Fig. 1 Yield of biocrude and solid residue over the lipid to protein ratio

this exponential correlation, the lowest value of 0.82% can be reached. Overall, the sum of biocrude and solid yield was also significantly increased when lipids were added to the feedstock mixture. Due to the non-polar nature of the lipids, i.e., their resulting fatty acids, they contribute largely to the DCM extracted biocrude [24]. The formation of solids during HTL is often explained by re-polymerization of carbohydrate degradation products, like furfural and hydroxymethylfurfural, into a carbonaceous material of high molecular weight [27]. Another reaction mechanism that is likely to contribute to the generation of solids is the Maillard reaction, which can form larger N-polymers named melanoidins. Peterson et al. identified melanoidins after the hydrothermal conversion of a binary mixture of glucose and glycine as a brownish N-containing polymer [28]. Additionally, the Mannich reaction pathway is presumed to form solid material by utilizing carbohydrate degradation products and amino compounds [29, 30]. Morphological and structural differences of the solid could not be identified. The ^{13}C-MAS NMR results show similar spectra of a solid obtained at an LtoP ratio of 0.00 and 1.00, displayed in S3. NMR analyses of solids obtained at larger LtoP ratios could not be performed because not enough material could be generated by the process.

3.2 Carbon and nitrogen content of feedstock mixtures and recovery into the resulting HTL-products phases

The investigated feedstock mixtures contain different carbon contents, as shown in Table 2. It can be noted that the C-, H-, and O-content for the different model feedstock is changing gradually, as the applied cellulose and lipid contain a different elemental composition due to their different chemical structure. In addition, the elemental contents of the resulting biocrude samples are given in the table. Interestingly, the C- and O-content do not change much, while the H-content is increasing and that of N and S is decreasing with higher LtoP ratios. Based on this data, the C- and N-recoveries in the different product phases are determined and displayed in Fig. 2. For the HTL process, a best possible C-recovery in the biocrude phase is desired for an efficient carbon utilization and its transfer to downstream processes for potential biofuel production. Vice versa, the N-recovery should be small, affecting downstream hydrotreating for denitrogenation [21].

In Fig. 2A the C-recovery and in (B) the N-recovery in the solid, biocrude and aqueous phases are shown. Likewise to the previously shown solid yield, the C- and N-recoveries in the solid show a similar downward trend. The recoveries

Table 2 Elemental content of model feedstocks and resulting biocrude samples. All values are given on a dry basis in wt.%

LtoP ratio	Feedstock mixture					Biocrude				
	C	H	N	S	O[a]	C	H	N	S	O[a]
0.00	44.60	6.80	5.00	0.57	43.03	73.28	8.08	6.40	1.00	11.25
0.34	48.50	7.43	5.00	0.57	38.50	74.70	9.30	5.10	0.70	10.20
0.66	52.17	8.03	5.00	0.57	34.23	75.10	9.90	4.50	0.50	10.00
1.00	56.07	8.67	5.00	0.57	29.70	74.37	10.53	3.90	0.57	10.63
1.34	59.97	9.30	5.00	0.57	25.17	74.60	11.20	3.20	0.40	10.60
1.66	63.63	9.90	5.00	0.57	20.90	74.50	11.70	2.70	0.40	10.70
2.00	67.53	10.53	5.00	0.57	16.37	74.93	12.18	2.43	0.33	10.15

[a]Calculated by difference

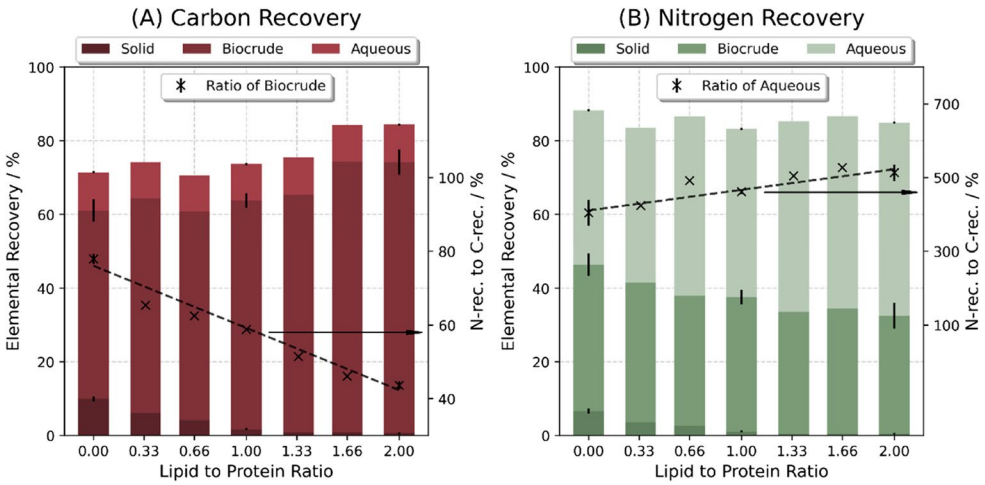

Fig. 2 Element recoveries of carbon (**A**) and nitrogen (**B**) into HTL-product phases over the lipid to protein ratio. Additionally, the ratio between N-rec. and C-rec. in the biocrude phase is plotted

significantly decrease from 9.75 to 0.58% for carbon and 6.85 to 0.46% for nitrogen, respectively. However, the element recoveries in the biocrude phase show different patterns. The addition of lipid to the model mixtures significantly increases the C-recovery of into the biocrude from 51.08 up to 73.64%, while the N-recovery is decreasing from 39.80 to 32.12%. In both figures, the ratio between these recoveries (N-recovery over C-recovery in the biocrude and aqueous) is plotted as a linear, dashed line. For the C-recovery, it can be noted that at a low LtoP range up to 77.92% of the recovered carbon account as nitrogen recovery. With the addition of lipids, this ratio can almost halved to a value of 43.60%. The element recoveries into the aqueous phase behave again differently. On the one hand, the C-recovery does not significantly change for the applied different feedstock mixtures with an average value of 10.13%. On the other hand, the N-recovery in the aqueous phase increases with the LtoP ratio starting at 41.92% for an LtoP ratio of 0.00 and rising up to 52.36% by addition of lipids. This aligns well with the decreasing N-recoveries in the biocrude. The N/C ratio shows a positive slope ranging from 404 to 513%, indicating an extraordinary higher transfer of N into the aqueous phase compared to the carbon distribution, supported by the addition of lipids. Summing up the elemental recoveries of all samples, a certain loss (difference to a total of 100%) can be identified. The larger losses of carbon can be explained by predominant decarboxylation reactions to CO_2 from carbohydrates [31]. N-losses are likely to occur due to the vacuum assisted separation process and the stripping of ammonia and other volatile amines, as described in the experimental section and elsewhere [21].

The effects of feedstock composition on the C- and N-content in the biocrude product can be visualized by a van Krevelen diagram, shown in Fig. 3. The ratio of N/C is plotted against that of H/C. In this graph, the feedstock mixtures are and different biocrude products are depicted. By the color code hand side, the different LtoP ratios are characterized. The typical removal of nitrogen from biogenic feedstocks via the hydrothermal conversion is likely to occur in form of ammonia (NH_3), which is indicated by deamination parallels in the graph. The biocrude samples originating from a high LtoP ratio are located in the upper left with high H/C and low N/C ratios. By reducing the LtoP ratio in the feedstock mixture, the biocrude samples show lower H/C values in combination with increased N/C values. It can be observed that the resulting points of the biocrude samples can be arranged in a straight line, with a slope of around 13, when a biocrude contains 1 mol less N but 12 mol more hydrogen. This goes along in a lower degree of aromatization of the biocrude. The mean distance Δ between the different product samples defined by the LtoP ratio are determined and shown on the right hand side of Fig. 3. The constant decrease of this mean distance over the LtoP ratio range can be translated as a decrease in aromaticity and is reasonable, as cellulose is likely to form aromatic species under these hydrothermal conditions [32]. Notably is the drop of this mean distance between the ratios of 0.00 to 0.33 and 0.33 to 0.66, indicating a strong effect of the addition of lipids.

3.3 Nitrogen recovery on a molecular level into different N-heteroatom species

Quantitative GC–MS analysis of the HTL-biocrude product obtained from the different feedstock mixtures was applied to explore the influence of the LtoP ratio on the formation of N-heteroaromatics and other N-heterocomounds. Representative compounds were chosen, based on a qualitative result obtained from a GC–MS chromatogram in scan mode of a sample with an LtoP ratio of 0.33, shown in S4. Compounds with the highest abundances were selected and compared with GCMS analysis of several studies, applying comparable feedstock and HTL procedure [5, 22, 24, 33, 34]. For these substance classes, the N-recoveries in the

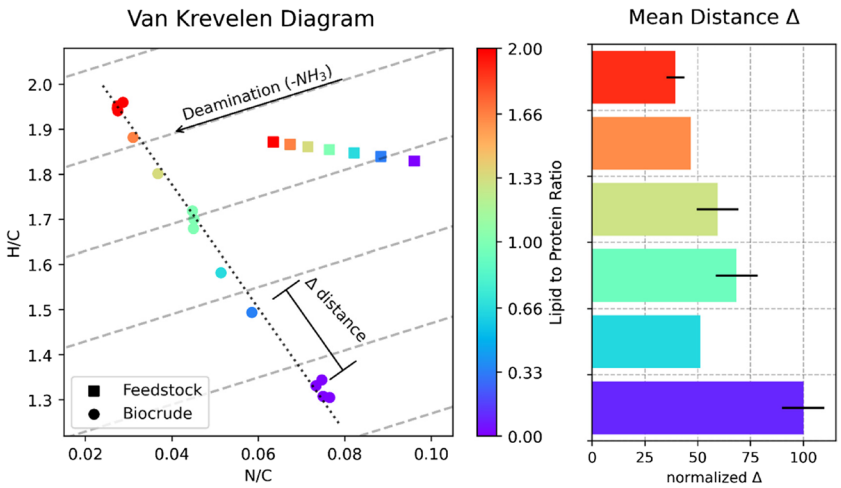

Fig. 3 Orientation of feedstock mixtures and the resulting biocrude products in van Krevelen diagram (N/C vs H/C) and mean distance between

biocrude from the different initial LtoP ratios and cellulose to protein (CtoP) ratios are shown in Fig. 4 and Fig. 5. The N-recoveries of representative N-heteroaromatics, pyrazines, indoles, and quinolines derivates are shown in Fig. 4. From the binary feedstock mixture of 2:1 cellulose and protein, a CtoP ratio of 2.00, a high quantity of pyrazine, is identified, and reflected in an N-recovery of 6.10%. With the addition of lipids and reduction of cellulose in the feed, the N-recoveries into pyrazines are drastically decreased to a sevenfold lower value of 0.87%. It seems that even higher LtoP ratios would not significantly affect the N-recovery in pyrazine structures. When no cellulose is present in the model feedstock, almost no pyrazines are identified.

The plot of the correlation of indole over the LtoP ratio range also follows an exponential decay, though the effect of an increasing LtoP ratio is weaker. The highest N-recovery in indoles is 2.69% at the LtoP ratio of 0.00 and CtoP ratio of 2.00, respectively. From a ternary mixed feedstock of 1:1:1 cellulose, proteins, and lipids, the N-recovery results in a value of 0.78%, which is further lowered to 0.44% in

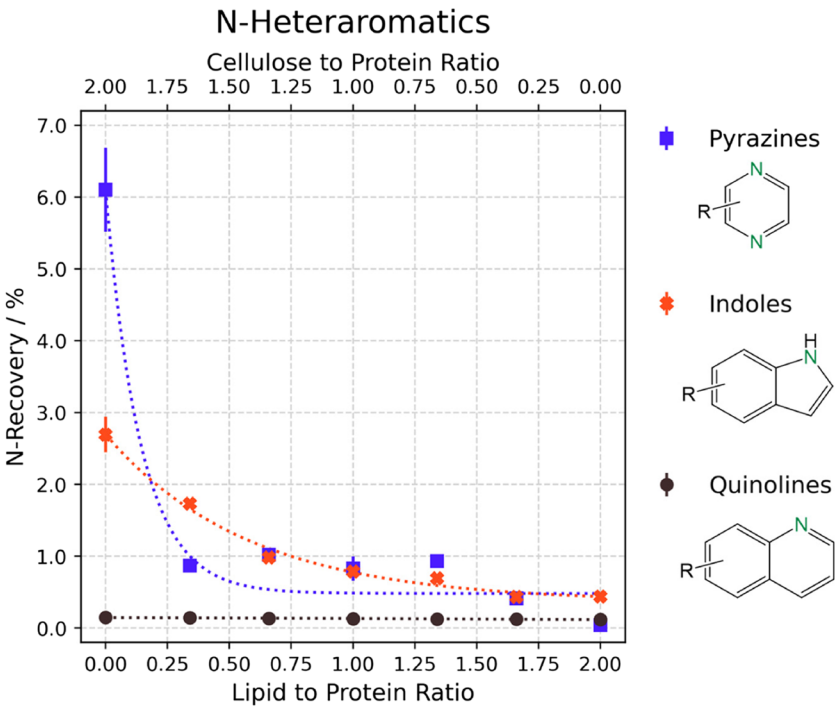

Fig. 4 Correlation of nitrogen recovery in dependence of the LtoP and CtoP ratio with pyrazines, indoles, and quinolones as representative N-heteroaromatics species in the biocrude products, obtained via HTL from different model feedstock mixtures

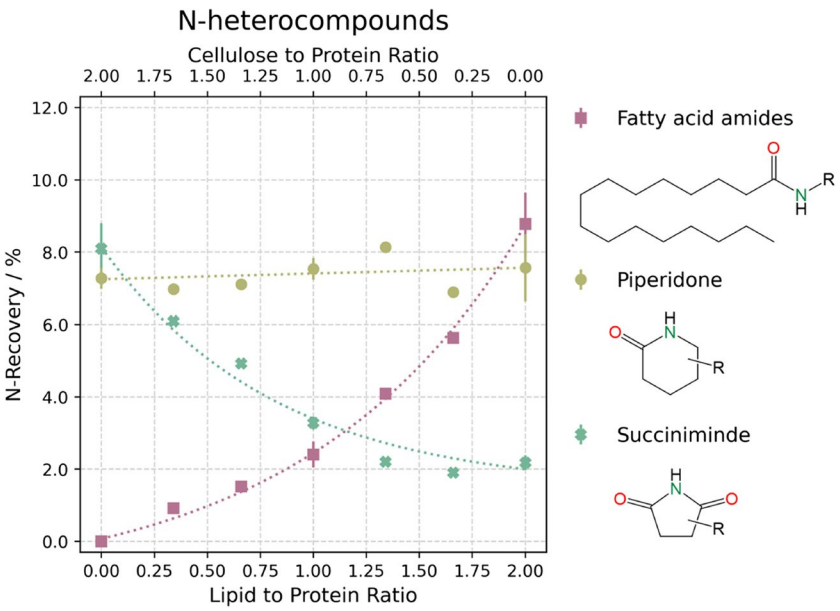

Fig. 5 Correlation of nitrogen recovery in dependence of the LtoP and CtoP ratio. N-heteroaliphatic and two non-aromatic N-heterocyclic species are determined in biocrude products, obtained via HTL from different model feedstock mixtures

the binary mixture of 2:1 lipids and proteins. The exponential decrease of both pyrazines and indoles agrees with the observed changes of the distance between the points representing the product mixtures in the van Krevelen diagram. The drastic suppression of pyrazine formation could be an explanation on the leap of the mean distance between the LtoP ratio 0.00 and 0.33. Moreover, it can be postulated that degradation products of cellulose serve as precursors for the formation of both pyrazines and indoles.

Quinoline derivates with a low molecular size could not be identified in relevant quantities. However, it cannot be excluded that these may appear in larger structures [35]. As the correlation shows, the summed values of these substances do not exceed 0.1% of the recovered nitrogen in the biocrude fraction.

To represent the generation of long-chain N-heteroaliphatic species, three palmitic (C16) and three stearic (C18) fatty acid amides (FAA) derivates were quantified, In addition, two non-aromatic N-heterocyclic species, 2-piperidon (5-ring lactam) and N-metylsuccinimide (4-ring imide), were analyzed. Likewise to the N-heteroaromatics, the N-recoveries of these species are determined and displayed with a correlation over the LtoP and inverted CtoP ratio range in Fig. 5. As no lipids were present in the binary feedstock mixture with a LtoP ratio of 0.00, no nitrogen is recovered in the form of FAA, as the precursing fatty acids are missing. With a rising LtoP ratio, the N-recovery in FAA is significantly rising to 8.77%. This phenomenon may explain the relatively modest reduction observed in the overall nitrogen recovery into the biocrude as previously determined. Herby the correlation curve is again following an exponential fitting. In contrast to the FAA, the N-recovery in succinimide decreases over the LtoP ratio range. With 8.09%, the highest recovery value is achieved with a binary cellulose protein feedstock. When fitting a curve to this data, it is following an exponential decrease. The lowest N-recovery is found at an LtoP ratio of 1.66 with a value of 1.90%. Similarly, this observation suggests a correlation with the degradation products of cellulose. The generation of piperidone seems not to be significantly affected by the changing feedstock mixture. The fitting is following a straight, almost horizontal line and the averaged N-recovery into this species is given at 7.36%.

3.4 Effect of propionic acid addition on biocrude yield and N-recovery

The effect of the addition of propionic acid on the N-recovery in the biocrude and aqueous phase products and on the N-heterocompounds defined above is shown in Fig. 6 by a change index graph. The change index is calculated by comparing the results of the corresponding experiment conducted at the same LtoP ratio or inverted CtoP ratio, but without the inclusion of propionic acid. It can be noted that the addition of propionic acid significantly lowers the N-recovery in the biocrude of model mixtures with an LtoP ratio of 0.00 and 0.33. Accordingly, the N-recovery in the aqueous phase significantly increases for all experiments, especially for those in the low LtoP ratio range, suggesting the formation of organic compounds like propanamide. Here it needs to be noted that the addition of propionic acid eventually led to a lower pH of the aqueous products, which prevents the above-described loss of ammonia by stripping during the separation procedure.

In the biocrude product, the change index describes in the following the N-recoveries on a molecular level. It can

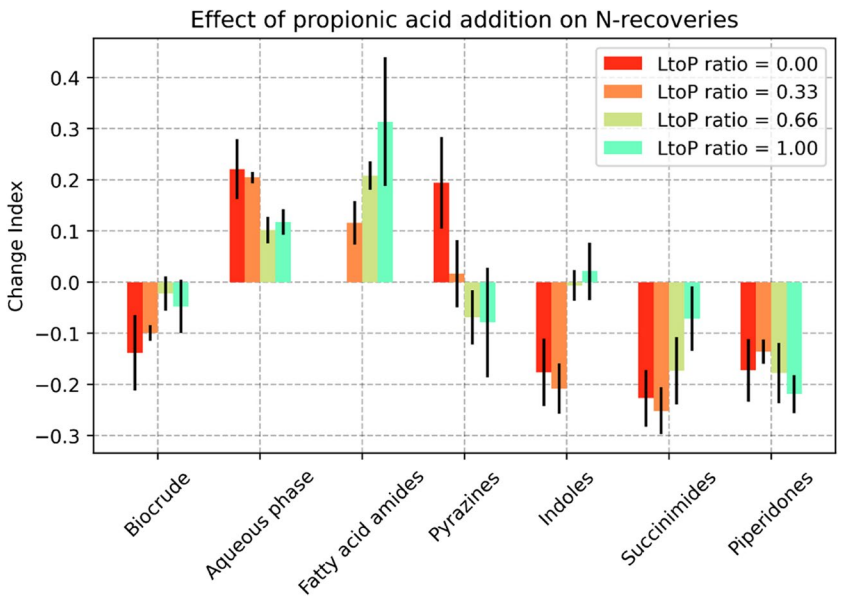

Fig. 6 The effect of the addition of propionic acid on the N-recovery into the HTL-products biocrude and aqueous phase and specific N-compounds, described by a Change Index

be observed that the formation of FAA increases when the model feedstock mixtures are liquefied in the presence of propionic acid. A proposed mechanism for the amidation reaction depends on a sequence of the protonation and deprotonation, which suggests the influence of the pH value. It needs to be noted that a strongly acidic or basic hydrothermal environment shows a contrary effect of the amide formation [36]. Formation of pyrazines is significantly increased at an LtoP ratio of 0.00. This is in agreement with findings, where the formation of diketopiperazine (DKP), a suggested pyrazine precursor, was significantly increased at lower pH and at comparable temperature [37]. At higher LtoP ratios, the formation of pyrazines is slightly reduced, as it was already strongly suppressed by the addition of lipids. In contrast, the formation of indoles is significantly reduced at lower LtoP ratios of 0.00 and 0.33, while at higher ratios essentially no effect was observed. Likewise to indole, the succinimide formation is reduced at lower LtoP ratios, while this effect becomes weaker with a LtoP ratio of 1.00. Both observations suggest that the addition of propionic acids can effectively intervene in the reaction pathway to these two compound classes. Due to a higher LtoP ratio, more fatty acids are present in the reaction system, which are comparable to carboxylic acids with a long carbon chain, therefore weakening the effect of this propionic, short-chain organic acid. Piperidone formation is reduced, indicated by the negative index, but no significant difference over the LtoP range can be determined, which reflects previous described behaviors in the baseline model system without the addition of propionic acid.

3.5 Reaction pathways forming N-heteroatomic compounds

Considering the above observed and described results, a simplified reaction scheme for the formation of the different N-heteroatom species is concluded and is discussed in detail.

The generation of N-heteroatomic compounds includes a variety of different possible reaction pathways. In Fig. 7, a scheme is shown derived from hydrothermal degradation of bovine serum albumin (protein), used as protein N-source in this study. This substance first hydrolyzes into different peptide oligomers, which are likely to degrade further into small amino compounds [38]. These can be considered intermediates for further consecutive reactions. Amino acids are likely to deaminate, yielding primarily ammonia or primary amines, but by decarboxylation reactions, secondary amines can be formed as well [33, 39]. In addition, these amino compounds of appropriate chain length can undergo internal ring closure. The 2-piperidone found in this study, is described as a product of 5-aminovaleric acid [40]. As presented by the N-recovery of this compound above, it is found that the cellulose and lipid content in the feedstock does not have a significant effect on the formation of this compound. Due to the 5-carbon atoms in the ring structure of 2-piperidone, it is assumed that it can only be formed from the cyclization of specific amino compounds. Otherwise, the formation of N-methylsuccinimide, which is assumed to be formed by several reaction mechanisms. On the one hand, amino compounds from peptide degradation can undergo internal ring closure. On the other hand, newly formed amino (amadori intermediates) derivates consist of a heteroatomic-5-ring containing four carbon atoms. The formation of succinimide was reported from succinic acid [41]. Succinic acid was found after the hydrothermal degradation of carbohydrates and presents one compound out of a pool of different reactive oxygenated species, such as hydroxymethylfurfural (HMF) or levulinic acid [42, 43]. These degradation products contain often a 4-carbon chain between two oxygen functional groups and are assumed to contribute to the formation of such heteroatomic-5-rings lactams and imides, including these 4 carbons.

The hydrothermal hydrolysis of cellulose into glucose and its subsequent conversion into different products at similar temperatures as applied in this experiment are described extensively in the literature [44, 45]. Via amination of these degradation products again, various species of these amadori intermediates are formed. Subsequent reactions can then lead to N-heteroaromatics like pyrazines or pyrrols. A pathway for pyrazine formation is proposed by Van Lancker et al. [46]. Dicarbonyls from carbohydrate degradation are aminated to α-aminocarbonyls, which condensate in turn to the corresponding pyrazines. Another proposed reaction mechanism is the formation of diketopiperazine as an intermediate with a subsequent reduction to pyrazine [47]. Other common N-heteroaromatics species are pyrroles and their indole derivates, containing one N, respectively. Pyrroles are likely to be formed from HMF via an aminated intermediate [48, 49]. In a subsequent step, these pyrroles can undergo cyclo-addition, forming indole derivates [50].

As demonstrated in the present study, the inclusion of lipids in the reaction mixture impedes the development of N-heteroaromatic compounds and the evaluated heterocyclic N-methylsuccinimide. Previous literature has reported that lipids have the ability to undergo hydrolysis, resulting in the formation of free fatty acids and glycerol [51]. These fatty acids may then react with free ammonia and amines to create stable fatty acid amides with various chain lengths and alkyl substituents [52]. This reaction pathway is in direct competition with the generation of amino intermediates from the amination of carbohydrate degradation products. Since fatty acid amides are stable and the formation of amino intermediates is suppressed, subsequent cyclization and rearrangement reactions into N-heteroaromatics are not occurring. Additionally by substituting cellulose with lipids in the

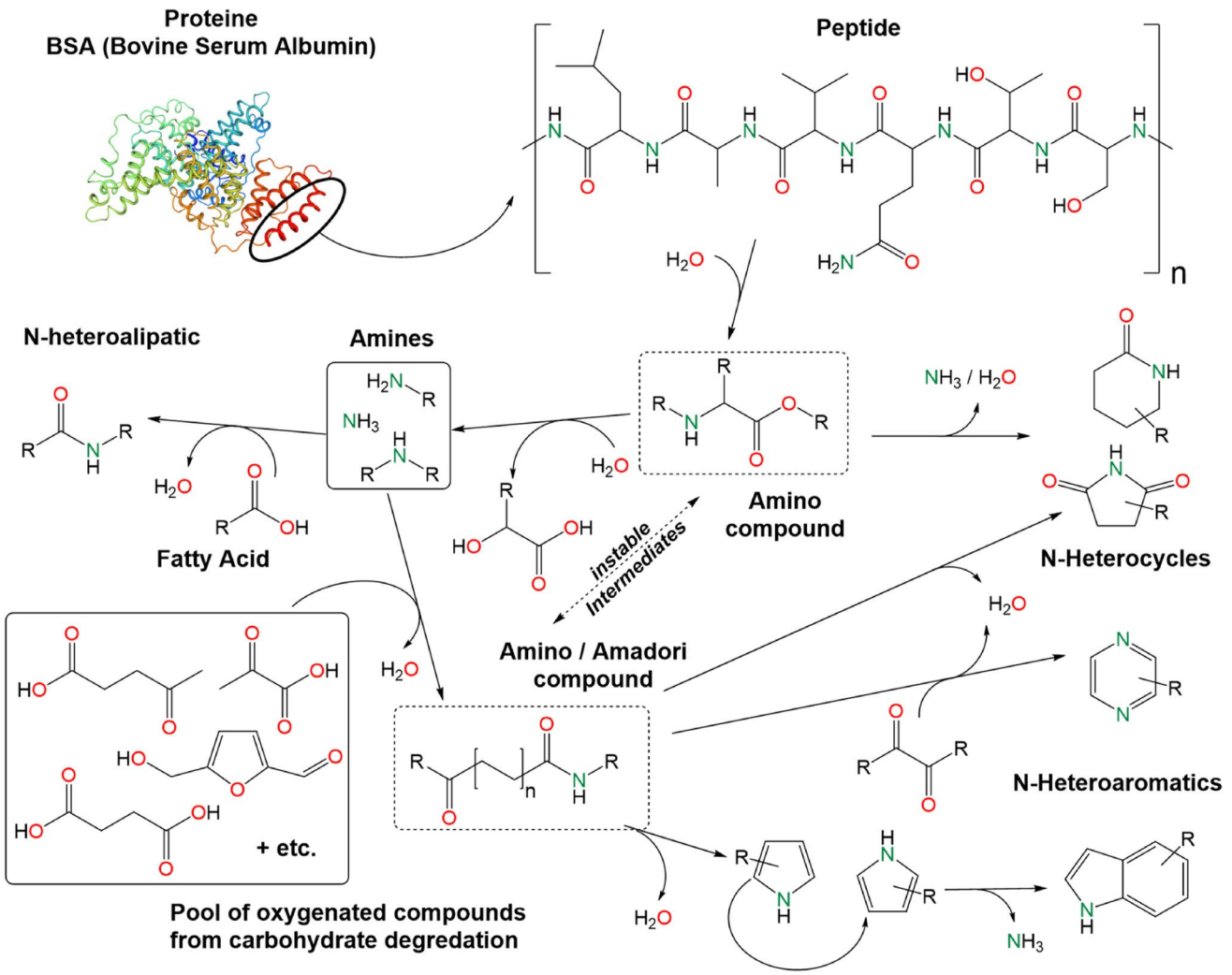

Fig. 7 Degradation of bovine serum albumin, the applied nitrogen source in this study, and possible formation pathways of different N-hetero-compounds

model feedstock mixture, the LtoP ratio increases and the CtoP ratio decreases. As less carbohydrates are present in the system and fewer of their degradation products, namely oxy-compounds are formed. Furthermore, more free fatty acids from lipid degradation are formed, making free amines more likely to form stable FAAs. Otherwise, the amines would react with an oxy-compound to form an N-heteroaromatic precursor [23]. For example, Inoue et al. identified a wide variety of N-heteroaromatic compounds like indoles and pyridines derivates after hydrothermal conversion of cellulose in an ammonia solution [53]. Their findings let suggest that free amines are highly reactive in a hydrothermal environment and are likely to react into the biocrude phase and form a large quantity and variety of different heterocyclic species [54]. These two reasons, firstly the competing amination and amidation reaction and secondly the addition of lipids reduces the amount of cellulose in the reaction mixture may explain the exponential regression curves observed in the recoveries of nitrogen into designated heteroaromatic species. Adding short-chain carboxylic acids, like propionic acid, can also compete with the formation of amino intermediates, but the resulting propanamide is highly water-soluble and is likely to found in the aqueous phase [47]. The inclusion of propionic acid or other suitable short-chain carboxylic acids emerges as a promising alternative, considering that real feedstocks typically exhibit low lipid-to-protein ratios. Moreover, the Maillard reaction between proteins and carbohydrates, or specifically the amination of intermediates in this context, appears to be the prevailing reaction pathway. Disrupting this reaction pathway represents a significant challenge.

4 Conclusion

In conclusion, the hydrothermal conversion of a model feedstock consisting of cellulose, a lipid component, and a protein component revealed the following key findings:

(1) The addition of lipids increased biocrude yield while reducing the formation of carbonaceous solids.
(2) Higher lipid content in the feedstock resulted in greater carbon recovery in the biocrude, accompanied by slightly lower nitrogen recovery.
(3) Increasing the lipid-to-protein ratio promoted the formation of fatty acid amides, suppressing the generation of N-heteroaromatic species, particularly pyrazines. Therefore, the majority of nitrogen recovery is allocated to aliphatic structures.
(4) It is crucial to sequester free amines in stable compounds to prevent amination of carbohydrate degradation products.
(5) Both lipids and short-chain carboxylic acids acted as amine "traps," forming N-aliphatic compounds in the biocrude or transferring nitrogen into the aqueous phase.

Future studies should employ high-resolution spectroscopy to validate the influence of lipids on N-heteroaromatic substance generation and identify relevant high molecular weight species. Furthermore, the investigation of real biomass feedstocks and the exploration of utilizing short-chain carboxylic acids obtained from the aqueous phase, coupled with the application of appropriate catalysts that have the potential to enhance the amidation pathway as amine traps, represent promising prospects for future advancements in this research field.

Acknowledgements The authors are grateful to Thomas Zevaco for conducting solid 13C-MAS NMR measurements. Aleksandra Kirchner (Institute of Catalysis and Technology Research (IKFT)) is acknowledged for her assistance in laboratory experiments.

Author contribution Conceptualization: [JZ, KR]; methodology: [JZ]; formal analysis and investigation: [JZ]; writing — original draft preparation: [JZ]; validation: [KR]; writing — review and editing: [KR, ND]; funding acquisition: [KR, ND]; supervision: [KR, ND].

Funding Open Access funding enabled and organized by Projekt DEAL. This research was funded by the European Union's Horizon 2020 research and innovation program under grant agreement No. 818413 (NextGenRoadFuel — Sustainable Drop-In Transport fuels from Hydrothermal Liquefaction of Low Value Urban Feedstocks).

Data availability Not applicable.

Declarations

Ethical approval Not applicable.

Competing interests The authors declare no competing interests.

References

1. Chowdhury H, Loganathan B (2019) Third-generation biofuels from microalgae: a review. Curr Opin Green Sustain Chem 20:39–44. https://doi.org/10.1016/j.cogsc.2019.09.003
2. Ramirez JA, Brown RJ, Rainey TJ (2015) A review of hydrothermal liquefaction bio-crude properties and prospects for upgrading to transportation fuels. Energies 8:6765–6794. https://doi.org/10.3390/en8076765
3. Kruse A, Dinjus E (2007) Hot compressed water as reaction medium and reactant. J Supercrit Fluids 39:362–380. https://doi.org/10.1016/j.supflu.2006.03.016
4. Biller P, Ross AB (2016) Production of biofuels via hydrothermal conversion. In: Handbook of biofuels production. Elsevier Ltd, pp 509-47. https://doi.org/10.1016/B978-0-08-100455-5.00017-5
5. Déniel M, Haarlemmer G, Roubaud A et al (2016) Energy valorisation of food processing residues and model compounds by hydrothermal liquefaction. Renew Sustain Energy Rev 54:1632–1652. https://doi.org/10.1016/j.rser.2015.10.017
6. SundarRajan P, Gopinath KP, Arun J et al (2021) Insights into valuing the aqueous phase derived from hydrothermal liquefaction. Renew Sustain Energy Rev 144:111019. https://doi.org/10.1016/j.rser.2021.111019
7. Leng L, Zhang W, Peng H et al (2020) Nitrogen in bio-oil produced from hydrothermal liquefaction of biomass: a review. Chem Eng J 401:126030. https://doi.org/10.1016/j.cej.2020.126030
8. Haider MS, Castello D, Rosendahl LA (2020) Two-stage catalytic hydrotreatment of highly nitrogenous biocrude from continuous hydrothermal liquefaction: a rational design of the stabilization stage. Biomass and Bioenergy 139:105658. https://doi.org/10.1016/j.biombioe.2020.105658
9. Haider MS, Castello D, Michalski KM, et al (2018) Catalytic hydrotreatment of microalgae biocrude from continuous hydrothermal liquefaction: heteroatom removal and their distribution in distillation cuts. Energies 11:. https://doi.org/10.3390/en11123360
10. Furimsky E (2000) Catalytic hydrodeoxygenation. Appl Catal A Gen 199:147–190. https://doi.org/10.1016/S0926-860X(99)00555-4
11. Leckel D (2006) Catalytic hydroprocessing of coal-derived gasification residues to fuel blending stocks: effect of reaction variables and catalyst on hydrodeoxygenation (HDO), hydrodenitrogenation (HDN), and hydrodesulfurization (HDS). Energy Fuels 20:1761–1766. https://doi.org/10.1021/ef060034d
12. Prado GHC, Rao Y, de Klerk A (2017) Nitrogen removal from oil: a review. Energy Fuels 31:14–36. https://doi.org/10.1021/acs.energyfuels.6b02779
13. Choudhary TV, Parrott S, Johnson B (2008) Understanding the hydrodenitrogenation chemistry of heavy oils. Catal Commun 9:1853–1857. https://doi.org/10.1016/j.catcom.2008.03.002

14. Prado GHC, de Klerk A (2016) Metals removal from metal-bridged molecules by acid treatment of oilsands bitumen and subfractions. Energy Fuels 30:20–30. https://doi.org/10.1021/acs.energyfuels.5b01482
15. Jarvis JM, Sudasinghe NM, Albrecht KO et al (2016) Impact of iron porphyrin complexes when hydroprocessing algal HTL biocrude. Fuel 182:411–418. https://doi.org/10.1016/j.fuel.2016.05.107
16. Kohansal K, Sharma K, Haider MS et al (2022) Hydrotreating of biocrude obtained from hydrothermal liquefaction of biopulp: effects of aqueous phase recirculation on the hydrotreated oil. Sustain Energy Fuels 6:2805–2822. https://doi.org/10.1039/D2SE00399F
17. Fan Y, Hornung U, Dahmen N, Kruse A (2018) Hydrothermal liquefaction of protein-containing biomass: study of model compounds for Maillard reactions. Biomass Convers Biorefinery 8:909–923. https://doi.org/10.1007/s13399-018-0340-8
18. Posmanik R, Cantero DA, Malkani A et al (2017) Biomass conversion to bio-oil using sub-critical water: study of model compounds for food processing waste. J Supercrit Fluids 119:26–35. https://doi.org/10.1016/j.supflu.2016.09.004
19. Yoo G, Park MS, Yang J-W, Choi M (2015) Lipid content in microalgae determines the quality of biocrude and energy return on investment of hydrothermal liquefaction. Appl Energy 156:354–361. https://doi.org/10.1016/j.apenergy.2015.07.020
20. Cheng F, Cui Z, Chen L et al (2017) Hydrothermal liquefaction of high- and low-lipid algae: bio-crude oil chemistry. Appl Energy 206:278–292. https://doi.org/10.1016/j.apenergy.2017.08.105
21. Zimmermann J, Raffelt K, Dahmen N (2021) Sequential hydrothermal processing of sewage sludge to produce low nitrogen biocrude. Processes 9:491
22. Croce A, Battistel E, Chiaberge S et al (2017) A model study to unravel the complexity of bio-oil from organic wastes. Chemsuschem 10:171–181. https://doi.org/10.1002/cssc.201601258
23. LeClerc HO, Atwi R, Niles SF et al (2022) Elucidating the role of reactive nitrogen intermediates in hetero-cyclization during hydrothermal liquefaction of food waste. Green Chem. https://doi.org/10.1039/D2GC01135B
24. Fan Y, Hornung U, Raffelt K, Dahmen N (2020) The influence of lipids on the fate of nitrogen during hydrothermal liquefaction of protein-containing biomass. J Anal Appl Pyrolysis 147:104798. https://doi.org/10.1016/j.jaap.2020.104798
25. VDI ev. (2010) VDI heat atlas. Springer, Berlin Heidelberg, Berlin, Heidelberg
26. Swiss-Model (2022) Crystaline Structure of Bovine Serum albumin - Bos taurus. https://swissmodel.expasy.org/repository/uniprot/P02769?template=3v03Accessed 23 May 2022
27. Jung D, Zimmermann M, Kruse A (2018) Hydrothermal Carbonization of Fructose: Growth Mechanism and Kinetic Model. ACS Sustain Chem Eng 6:13877–13887. https://doi.org/10.1021/acssuschemeng.8b02118
28. Peterson AA, Lachance RP, Tester JW (2010) Kinetic evidence of the maillard reaction in hydrothermal biomass processing: glucose-glycine interactions in high-temperature, high-pressure water. Ind Eng Chem Res 49:2107–2117. https://doi.org/10.1021/ie9014809
29. Chen X, Peng X, Ma X, Wang J (2019) Investigation of Mannich reaction during co-liquefaction of microalgae and sweet potato waste. Bioresour Technol 284:286–292. https://doi.org/10.1016/j.biortech.2019.03.136
30. Alhnidi M, Straten JW, Nicolae SA et al (2022) Thermal treatment versus hydrothermal carbonization: how to synthesize <scp>nitrogen-enriched</scp> carbon materials for energy storage applications? Int J Energy Res 46:1622–1636. https://doi.org/10.1002/er.7275
31. Gollakota A, Savage PE (2018) Hydrothermal liquefaction of model food waste biomolecules and ternary mixtures under isothermal and fast conditions. ACS Sustain Chem Eng 6:9018–9027. https://doi.org/10.1021/acssuschemeng.8b01368
32. Kruse A, Dahmen N (2017) Hydrothermal biomass conversion: quo vadis? J Supercrit Fluids 134:114–123. https://doi.org/10.1016/j.supflu.2017.12.035
33. Sheehan JD, Savage PE (2017) Molecular and lumped products from hydrothermal liquefaction of bovine serum albumin. ACS Sustain Chem Eng 5:10967–10975. https://doi.org/10.1021/acssuschemeng.7b02854
34. Sayegh A, Merkert S, Zimmermann J et al (2022) Treatment of hydrothermal-liquefaction wastewater with crossflow UF for oil and particle removal. Membranes (Basel) 12:255. https://doi.org/10.3390/membranes12030255
35. Zimmermann J, Chiaberge S, Iversen SB et al (2022) Sequential extraction and characterization of nitrogen compounds after hydrothermal liquefaction of sewage sludge. Energy Fuels 36:14292–14303. https://doi.org/10.1021/acs.energyfuels.2c02622
36. Fu X, Liao Y, Glein CR et al (2020) Direct synthesis of amides from amines and carboxylic acids under hydrothermal conditions. ACS Earth Sp Chem 4:722–729. https://doi.org/10.1021/acsearthspacechem.0c00009
37. Kitadai N (2014) Thermodynamic prediction of glycine polymerization as a function of temperature and pH consistent with experimentally obtained results. J Mol Evol 78:171–187. https://doi.org/10.1007/s00239-014-9616-1
38. Rogalinski T, Herrmann S, Brunner G (2005) Production of amino acids from bovine serum albumin by continuous sub-critical water hydrolysis. J Supercrit Fluids 36:49–58. https://doi.org/10.1016/j.supflu.2005.03.001
39. Abdelmoez W, Yoshida H, Nakahasi T (2010) Pathways of amino acid transformation and decomposition in saturated subcritical water conditions. Int J Chem React Eng 8:. https://doi.org/10.2202/1542-6580.1903
40. Islam MN, Kaneko T, Kobayashi K (2003) Reaction of amino acids in a supercritical water-flow reactor simulating submarine hydrothermal systems. Bull Chem Soc Jpn 76:1171–1178. https://doi.org/10.1246/bcsj.76.1171
41. Déniel M, Haarlemmer G, Roubaud A et al (2017) Hydrothermal liquefaction of blackcurrant pomace and model molecules: understanding of reaction mechanisms. Sustain Energy Fuels 1:555–582. https://doi.org/10.1039/c6se00065g
42. Kruse A, Gawlik A (2003) Biomass conversion in water at 330–410 °C and 30–50 MPa. Identification of key compounds for indicating different chemical reaction pathways. Ind Eng Chem Res 42:267–279. https://doi.org/10.1021/ie0202773
43. Weingarten R, Conner WC, Huber GW (2012) Production of levulinic acid from cellulose by hydrothermal decomposition combined with aqueous phase dehydration with a solid acid catalyst. Energy Environ Sci 5:7559–7574. https://doi.org/10.1039/c2ee21593d
44. Sinag A, Kruse A, Schwarzkopf V (2003) Key compounds of the hydropyrolysis of glucose in supercritical water in the presence of K2CO3. Ind Eng Chem Res 42:3516–3521. https://doi.org/10.1021/ie030079r
45. Remón J, Laseca M, García L, Arauzo J (2016) Hydrogen production from cheese whey by catalytic steam reforming: preliminary study using lactose as a model compound. Energy Convers Manag 114:122–141. https://doi.org/10.1016/j.enconman.2016.02.009
46. Van Lancker F, Adams A, De Kimpe N (2010) Formation of pyrazines in Maillard model systems of lysine-containing dipeptides. J Agric Food Chem 58:2470–2478. https://doi.org/10.1021/jf903898t
47. Madsen RB, Biller P, Jensen MM et al (2016) Predicting the chemical composition of aqueous phase from hydrothermal liquefaction of model compounds and biomasses. Energy Fuels 30:10470–10483. https://doi.org/10.1021/acs.energyfuels.6b02007

48. Lichtenthaler FW (2002) Unsaturated O- and N-heterocycles from carbohydrate feedstocks. Acc Chem Res 35:728–737. https://doi.org/10.1021/ar010071i
49. Wozniak B, Tin S, de Vries JG (2019) Bio-based building blocks from 5-hydroxymethylfurfural via 1-hydroxyhexane-2,5-dione as intermediate. Chem Sci 10:6024–6034. https://doi.org/10.1039/C9SC01309A
50. Katritzky AR, Luxem FJ, Murugan R et al (1992) Aqueous high-temperature chemistry of carbo- and heterocycles. 19. Pyrroles and indoles Energy & Fuels 6:450–455. https://doi.org/10.1021/ef00034a014
51. Fan Y, Hornung U, Dahmen N (2022) Hydrothermal liquefaction of sewage sludge for biofuel application: a review on fundamentals, current challenges and strategies. Biomass and Bioenergy 165:106570. https://doi.org/10.1016/j.biombioe.2022.106570
52. Chiaberge S, Leonardis I, Fiorani T et al (2013) Amides in bio-oil by hydrothermal liquefaction of organic wastes: a mass spectrometric study of the thermochemical reaction products of binary mixtures of amino acids and fatty acids. Energy Fuels 27:5287–5297. https://doi.org/10.1021/ef4009983
53. Inoue S, Okigawa K, Minowa T, Ogi T (1999) Liquefaction of ammonia and cellulose: effect of nitrogen/carbon ratio in the feedstock. Biomass Bioenerg 16:377–383. https://doi.org/10.1016/S0961-9534(99)00003-3
54. Jensen CU, Rosendahl LA, Olofsson G (2017) Impact of nitrogenous alkaline agent on continuous HTL of lignocellulosic biomass and biocrude upgrading. Fuel Process Technol 159:376–385. https://doi.org/10.1016/j.fuproc.2016.12.022